

Controlled electronic coupling between two quantum wells: A photoemission study of noble-metal systems

W. E. McMahon, M. A. Mueller,* T. Miller, and T.-C. Chiang

*Department of Physics, University of Illinois at Urbana-Champaign, 1110 West Green Street, Urbana, Illinois 61801-3080
and Materials Research Laboratory, University of Illinois at Urbana-Champaign, 104 South Goodwin Avenue,
Urbana, Illinois 61801-2902*

(Received 27 September 1993)

Double quantum wells are grown on Au(111) and Cu(111) substrates using Ag as the well material and either Cu or Au as a barrier material. The barrier thickness is varied to change the coupling between the two wells, and the resulting double-quantum-well states are probed with photoemission. In the limit of a very thick barrier, the coupling is eliminated, and the allowed states become those of two independent wells. When the barrier thickness is reduced to zero, the two quantum wells combine to form a single well. Between these two limits, the observed evolution of the binding energies and intensities is compared with the predictions of a simple theoretical model based upon Bloch wave functions. The effects of smoothing the barrier potential are studied by annealing a Au barrier sample, allowing atomic interdiffusion between the Au barrier and the Ag wells.

I. INTRODUCTION

The study of epitaxially grown metallic multilayers is a field of increasing interest.¹ The physics and synthesis of such systems are relevant to the development of quantum devices based on small-size and proximity-coupling effects. Present layer deposition technologies allow precise control of the sample configuration with atomic layer resolution. This capability of "atomic layer engineering" facilitates studies of fundamental quantum-mechanical effects in various layer configurations.

This work is a demonstration of electronic-coupling effects between two Ag(111) quantum wells. It is well established that thin layers deposited on a substrate, with or without additional overlayers, can exhibit quantum-well states due to confinement of the valence electrons by the potential steps at the two boundaries.²⁻⁶ In our study, we prepared two Ag(111) quantum wells of equal thickness separated by either a Au(111) or Cu(111) barrier. If the barrier thickness is sufficiently small, the two wells can couple electronically via evanescent waves in the barrier, and the wave functions of the valence electrons will occupy both wells.⁷ In our experiment, we use angle-resolved photoemission to study the energy positions and photoemission intensities of these double-well states as functions of the barrier thickness. In particular, we follow the evolution from a combined single well, where the barrier thickness is zero, to two independent wells, where the barrier thickness is large. Thus, the two limiting cases are just single wells differing by a factor of two in thickness. An examination of these limiting cases allows a simple qualitative interpretation of the data to be made. For a more detailed quantitative description, a theoretical model based on Bloch wave functions was used. These calculations are straightforward because the relevant band structures of the noble metals are fairly simple, and can be modeled analytically with a good degree of precision.

Although Ag is always used as a well material in this study, the substrates and barriers for these samples can be made using different combinations of Au and Cu with similar results. This demonstrates that the effects to be reported are not unique to just one system. In fact, the similarity among these different systems is expected because the underlying physics is the same. In addition, we have performed an annealing experiment for a case with a Au barrier. The annealing causes the Ag and Au to interdiffuse, smoothing the barrier potential, which in turn modifies the eigenstates of the system.

II. EXPERIMENTAL DETAILS

The photoemission measurements were performed at the Synchrotron Radiation Center of the University of Wisconsin-Madison. A hemispherical electron energy analyzer with a 3° full acceptance angle was used to collect the photoemission spectra. A normal emission geometry was employed in all measurements, so only states with a zero momentum component parallel to the surface were detected. In other words, this was essentially a one-dimensional experiment. The various sample configurations were fabricated *in situ* by molecular-beam epitaxy. Substrate cleaning, film deposition, and sample characterization followed standard procedures.²⁻⁴ Sample preparation in this experiment was particularly time consuming, since for each different barrier thickness the entire sample had to be redeposited.

III. RESULTS AND DISCUSSION

A. Results for Au(111)/Ag₁₀/Au_y/Ag₁₀

We will begin with a detailed study of a double quantum well grown using Au for both the substrate and the barrier. On a Au(111) substrate we deposited a ten monolayer (ML) Ag well followed by a Au barrier and a second 10-ML Ag well. For brevity, we will denote this

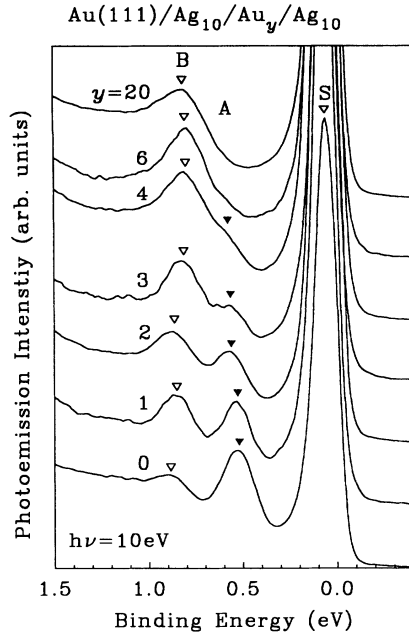


FIG. 1. Normal-emission photoemission spectra taken with a photon energy of $h\nu = 10$ eV for $\text{Au}(111)/\text{Ag}_{10}/\text{Au}_y/\text{Ag}_{10}$ with various barrier thicknesses y as indicated. A large surface state (S) and two smaller double-quantum-well states (A and B) are indicated by triangles. The binding-energy scale is referred to the Fermi level.

system as $\text{Au}(111)/\text{Ag}_{10}/\text{Au}_y/\text{Ag}_{10}$, where y is the thickness of the Au barrier in ML. Figure 1 shows a set of normal emission spectra taken with a photon energy $h\nu = 10$ eV for various values of y . When y is zero (bottom spectrum), the system is a single 20-ML well. When y is large (top spectrum), only states in the outer well are observed with photoemission because of its finite photoelectron escape depth, so the system resembles a single 10-ML well. These results for Au/Ag single quantum wells are already well known and documented.^{2,3,8}

In each spectrum, one sees an intense peak just below the Fermi level corresponding to a surface state within the sp band gap of Ag. This is known as the L -gap surface state. Since it is localized near the surface, it is not appreciably affected by the buried interfaces. In the bottom spectrum, one sees two additional peaks at about 0.5 and 0.9 eV, corresponding to single-quantum-well states with quantum numbers $n = 1$ and 2, respectively. As discussed in a previous publication,² quantum-well states for Ag on Au(111) are only observed between the Au(111) band edge at 1.1 eV and the Ag(111) band edge at 0.33 eV. This explains why we do not see additional peaks ($n = 3, 4, \dots$) at higher binding energies. The top spectrum shows just one quantum-well peak ($n = 1$) at about 0.8 eV. This is because a 10-ML single well supports only one state in the energy range of 0.33–1.1 eV. (Recall that in the limit of a thick barrier, the double-quantum-well resembles a single well.) If the thickness of the Ag well were varied continuously from an initial thickness of 20

ML (bottom spectrum) to a final thickness of 10 ML (top spectrum), the $n = 1$ quantum-well state would evolve continuously from 0.5 to 0.8 eV. Likewise, the $n = 2$ state would evolve continuously, from its initial position of 0.9 eV (bottom spectrum) to higher binding energies, disappearing as it crossed the Au band edge at 1.1 eV. The important point here is that when the quantum-well thickness is varied continuously, the quantum-well states evolve continuously, *maintaining their quantum number designations*, as demonstrated in previous studies of single wells.^{2–6,8} A reduction of quantum-well thickness by one-half (from 20 to 10 ML in this case) results in a corresponding reduction of the allowed k values, so the number of observable states will generally also be reduced by one-half.

In the present experiment, the bottom and top spectra in Fig. 1 are *not* connected by a continuous change in quantum-well thickness, and the behavior indicated by the intermediate spectra in Fig. 1 is obviously *not* a simple continuous energy evolution of the $n = 1$ state. Rather, the data in Fig. 1 shows the original $n = 1$ peak in the bottom spectrum disappearing as y increases, while the original $n = 2$ state gradually evolves into the $n = 1$ state. This switching of quantum numbers is a consequence of the way in which the two limiting cases are connected. This is an interesting demonstration of different pathways between the same set of limiting cases following *qualitatively* different evolutions. The observed switching of quantum numbers does not violate any fundamental laws of physics, and is frequently observed in the more familiar case of an anticrossing of two energy levels. If the $n = 3, 4, \dots$ states were observable in the present experiment, they would behave similarly; i.e., as y increases the $n = 3$ peak would disappear, while the $n = 4$ state would evolve into the $n = 2$ state in the outer (10 ML) well, etc. So, as the barrier separating the two wells is made thicker, every other peak disappears from the spectra, since only half of the states will remain in the outer well where they can be observed with photoemission. Although the present case is highly academic, it provides an interesting example of “electronic state engineering.”

B. Theoretical modeling and interpretation

One can understand the above results based on an analogy to the simple one-dimensional particle-in-a-box problem commonly described in quantum-mechanics textbooks. Some complications arise for the real system because the crystal potential causes the sp wave function to oscillate rapidly with a “holelike” dispersion in the energy range of interest.^{2,3,6} Nevertheless, there is a great deal of similarity if one considers only the envelope function of the quantum-well state and inverts the energy scale to account for the holelike dispersion. In the following, we will show results from our model calculation, make a comparison to the experimental results, and finally present a qualitative interpretation based on this analogy.

The details and parameters of our model calculation can be found in previous publications regarding single wells and other layer configurations.^{3,4,7,9} Briefly, we de-

scribe the wave functions in Ag and Au using a two-band model, with an effective mass correction to account for multiband effects. The wave functions are analytic functions of energy, fully determined by the experimentally measured dispersion curves of Ag and Au. We assume that the Ag-Au interface is infinitely sharp, so the Ag and Au wave functions extend right to the boundaries. The vacuum barrier is modeled with a linear potential to account for the surface dipole layer. Its slope is the only free parameter in the model, and it is adjusted to yield the correct surface-state energy. The wave functions in the different regions are either propagating or evanescent. They are matched at the boundaries, and bound-state solutions are found by setting $\Psi=0$ both deep in the substrate and far away from the surface in vacuum. This results in discrete eigenstates corresponding to the double-well system. Shown in Fig. 2 are probability density functions $|\Psi|^2$ for the two eigenstates *A* and *B* for a few representative values of y . These correspond to peaks *A*

and *B* in Fig. 1. The calculated eigenenergies as a function of y are shown in Fig. 3 using circles connected by smooth dashed curves. The expected variations of the photoemission intensities for these states can be calculated as a function of y using a very simple model:

$$I \propto \int_{-\infty}^0 |\Psi|^2 \exp(z/\lambda) dz + \int_0^{\infty} |\Psi|^2 dz ,$$

where z is the distance measured from the surface ($z < 0$ for inside the crystal) and $\lambda=20 \text{ \AA}$ is the photoelectron escape depth. The predicted intensities are indicated by the area of each circle shown in Fig. 3. The photoelectron escape depth is essentially the probing depth of photoemission, which can be varied by changing the photon energy. In our case, this probing depth (20 \AA) is less than the outer well thickness (23.6 \AA), so a state's photoemission peak intensity is derived mostly from emission from the outer well. This is why states confined to the inner well are invisible to photoemission.

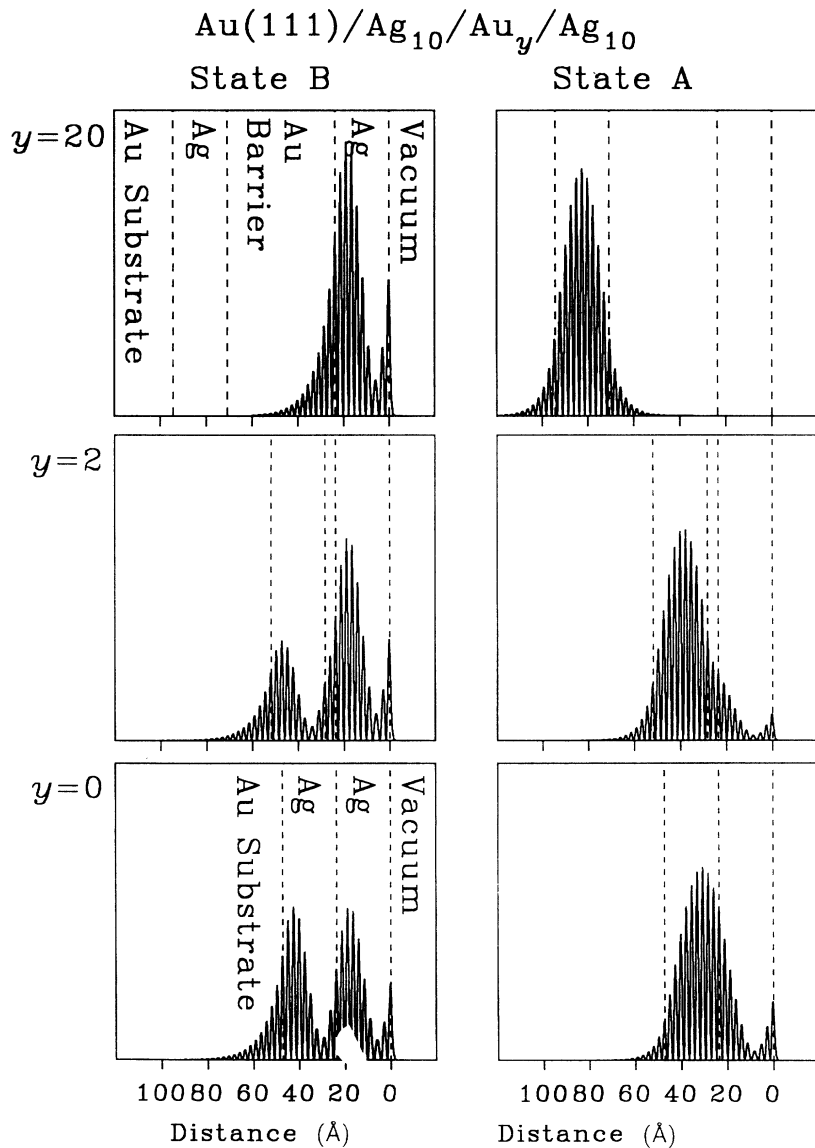


FIG. 2. Probability density functions $|\Psi|^2$ of states *A* and *B* for a few representative Au barrier thicknesses.

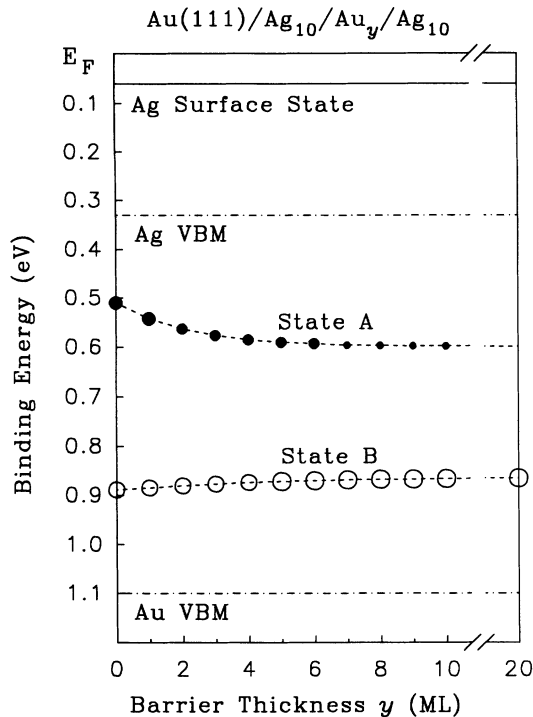


FIG. 3. Theoretically predicted double-quantum-well states for $\text{Au}(111)/\text{Ag}_{10}/\text{Au}_y/\text{Ag}_{10}$ as a function of the barrier thickness y . The binding energies of these states (*A* and *B*) are plotted using circles which are connected by smooth dashed curves. Expected photoemission peak intensity is proportional to the area of each circle. For reference, the Ag surface state and the Ag and Au valence-band maxima (VBM) are indicated.

The experimentally observed intensities and peak positions are shown in Fig. 4, where again the area of each circle is proportional to the intensity. The theoretical peak positions, indicated by the dashed curves, are reproduced from Fig. 3 for easy comparison. There is a good overall agreement between the experiment and theory. The main features are that the two states *A* and *B* show very small dispersions as a function of y , and that the intensity of peak *A* decreases as y increases, whereas the intensity of peak *B* increased by about a factor of 2 to a saturation value.

These results can be understood qualitatively with the aid of an analogy to the case of the particle-in-a-box problem. The wave functions shown in the bottom panels in Fig. 2 are for a single 20-ML well. State *A* here corresponds to the $n=1$ state. Ignoring the rapid oscillations caused by the crystal potential, one sees an envelope function with a large hump, or antinode, within the combined single well. Likewise, state *B*, corresponding to the $n=2$ state, shows two humps separated by a node at about the midpoint of the well. One can easily show that this is a general result for a single well; the quantum number n is just the number of humps, or antinodes, in the well. This is very similar to the particle-in-a-box problem. There exists, however, an important difference. Both states *A* and *B* in Fig. 2 appear to show an additional node right next to the surface, giving rise to a small an-

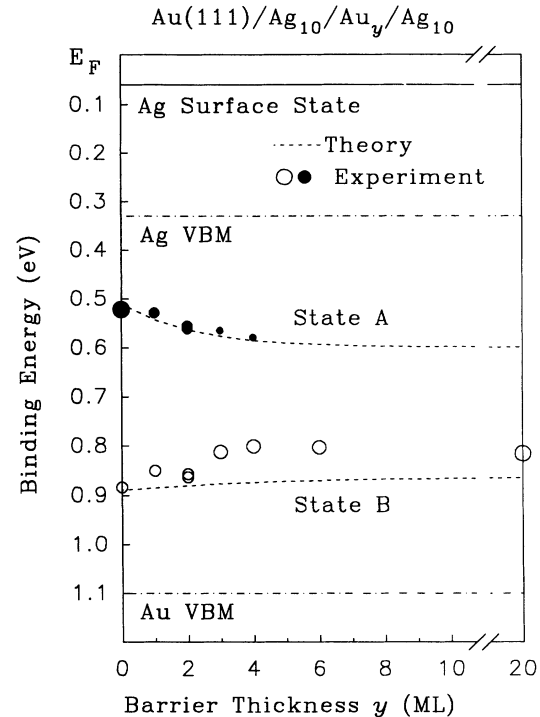


FIG. 4. Experimentally observed double-quantum-well states for $\text{Au}(111)/\text{Ag}_{10}/\text{Au}_y/\text{Ag}_{10}$ as a function of the barrier thickness y (taken from the spectra in Fig. 1; $h\nu=10$ eV). The observed binding energies of the states *A* and *B* are plotted as circles with the area proportional to the photoemission intensity. For reference, the theoretical binding energies shown as dashed curves in Fig. 3 are reproduced here. The Ag surface state and the Ag and Au VBM are also indicated.

tinode at the surface. This can be related to the presence of a surface state, which has no analog in the problem of a particle in a box. This extra node (surface node) pushes the $n=1$ state deeper below the surface, so the main hump is mostly concentrated in the inner half of the combined well. Thus, the presence of the surface breaks the symmetry between the two wells.

In the limit of very large y , the system becomes two independent wells, each with a width 10 ML. The upper panels of Fig. 2 illustrate the situation. Here, one sees that each well supports its own $n=1$ state, with one large antinode. The energies of the two $n=1$ states are different due to the different boundary conditions. Our calculations show that the original $n=1$ state for $y=0$ (lower right panel in Fig. 2) evolves into the $n=1$ state in the inner well when y becomes large (upper right panel in Fig. 2). It does not evolve into the outer well state with $n=1$. Why not? This has to do with the symmetry of the system. As mentioned above, the surface node pushes the main hump of state *A* for $y=0$ mostly into the inner half of the combined well. Consequently, the envelope function has a negative slope at the midpoint of the combined well. As the barrier is added, the envelope function in the inner well continues to have a negative slope at this boundary, because the wave function in the barrier is evanescent in nature. So, an antinode is maintained in

the inner well as y increases, and when y becomes large, state A must evolve into the inner well state. The envelope function in the outer half of the well, in contrast, has an initial slope at the boundary that is incompatible in sign with that of the evanescent wave in the barrier as y increases. Therefore, a solution to the wave equation cannot be maintained in the outer well. A similar argument can be made for state B .

Thus, the $n=1$ state for $y=0$ evolves into the $n=1$ state in the inner well for increasing y (state A), while the $n=2$ state evolves into the $n=1$ state in the outer well (state B). Because the inner-well state cannot be detected by photoemission when y is large, the original $n=1$ peak gradually disappears from the photoemission spectra for increasing y , as seen in Fig. 1. Also, the concentration of state B into the outer well as y changes from 0 to ∞ will lead to roughly a factor of two increase of $|\Psi|^2$ for state B in the outer well (see Fig. 2), causing the photoemission intensity of peak B to increase by roughly the same factor, as seen in Fig. 1.

C. Results for Cu(111)/Ag₁₀/Au_y/Ag₁₀ and Cu(111)/Ag₁₀/Cu_y/Ag₁₀

We have tried the same experiment using Cu(111) as the substrate. The electronic properties of Cu(111) are fairly similar to Au(111). The only major difference is that the band edge of Cu(111) is at about 0.85 eV, as compared to 1.1 eV for Au(111).³ Quantum-well states therefore exist in a reduced energy range of between 0.33 and 0.85 eV. For binding energies greater than 0.85 eV, only resonances can exist. However, the large lattice mismatch between Ag and Cu apparently causes an enhanced decoupling between the electronic states. Thus, well-defined resonances have been observed for Ag quantum wells on Cu(111) even for binding energies larger than 0.85 eV.^{3,4} Figure 5 shows a set of photoemission data for Cu(111)/Ag₁₀/Au_y/Ag₁₀. The results are very similar to those shown in Fig. 1, as expected.

We have also tried Cu as the barrier layer; the results for Cu(111)/Ag₁₀/Cu_y/Ag₁₀ are shown in Fig. 6. Again, the results are very similar to those shown in Figs. 1 and 5. These results demonstrate that the phenomena discussed above are not unique to just one system.

D. Annealing experiment

We have taken a limited set of data on the annealing behavior of double-well systems. The data set is rather limited, because annealing can cause significant interdiffusion, ultimately ruining the substrates. Obviously, we did not wish to destroy our substrates. As mentioned above, the idea is to modify (smooth out) the barrier potential via thermally induced atomic interdiffusion¹⁰ and see what happens to the double-well states. For this experiment, we chose the configuration Cu(111)/Ag₁₀/Au₂/Ag₁₀. The Cu(111) substrate was chosen because Ag and Cu do not intermix even at elevated temperatures, so the Ag-Cu interface should remain sharp after annealing. The barrier material was chosen to be Au, because Ag and Au are easily inter-

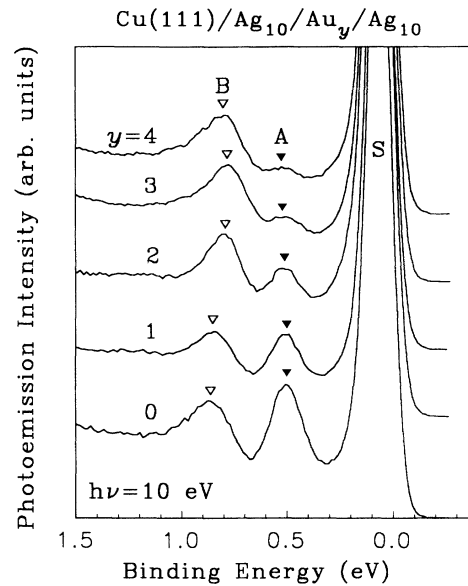


FIG. 5. Normal-emission photoelectron spectra taken with a photon energy of $h\nu=10$ eV for Cu(111)/Ag₁₀/Au_y/Ag₁₀ with various barrier thicknesses y as indicated. A large surface state (S) and two smaller double-quantum-well states (A and B) are indicated. The binding-energy scale is referred to the Fermi level.

mixed by thermal annealing. In the experiment, each annealing cycle involved heating the sample for 10 min to 300°C.

Figure 7 shows the results for 0, 1, and 2 cycles of annealing. The original sample shows two double-well states A and B as indicated by the triangles, and maybe a

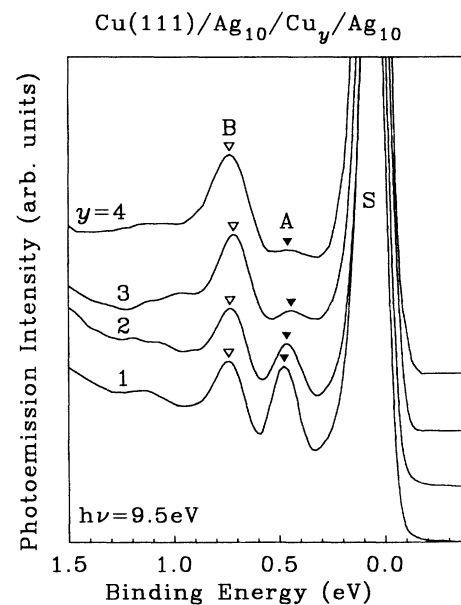


FIG. 6. Normal-emission photoelectron spectra taken with a photon energy of $h\nu=9.5$ eV for Cu(111)/Ag₁₀/Cu_y/Ag₁₀ with various barrier thicknesses y as indicated. A large surface state (S) and two smaller double-quantum-well states (A and B) are indicated. The binding-energy scale is referred to the Fermi level.

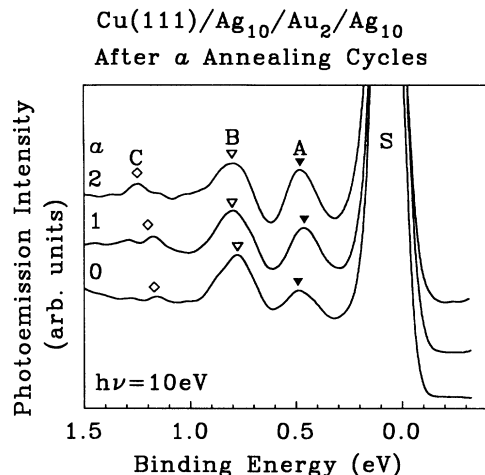


FIG. 7. Normal-emission photoelectron spectra taken with a photon energy of $h\nu = 10\text{ eV}$ for Cu(111)/Ag₁₀/Au₂/Ag₁₀ after 0–2 annealing cycles. During each cycle the sample was heated for 10 min to 300 °C. A large surface state (S) and three smaller double-quantum-well states (A–C) are indicated. The binding-energy scale is referred to the Fermi level.

hint of a third (resonance) state C. The annealing causes the intensity of states A and C to increase. This is easily understood. The original Au barrier causes states A and C to be partially pushed into inner wells. The annealing causes a dilution of the barrier, moving the system more toward a single-well configuration. Thus, states A and C should regain their intensities.

IV. SUMMARY

This study is an illustration of electronic-coupling effects through a barrier in a double-quantum-well sys-

tem. The sample consists of two wells of equal thickness separated by a barrier of variable width. As the barrier width is increased, the system evolves from a single 20-ML well into two independent 10-ML wells. In this process, single-well states with odd (even) quantum numbers n evolve into states in the inner (outer) well. This is verified in our experiment by measuring the photoemission peak intensities, which are sensitive to the spatial localization of the states relative to the surface. The results of theoretical model utilizing Bloch wave functions show good agreement with the experiment. A simple interpretation, taking into account the asymmetry of the system due to the surface, is offered.

ACKNOWLEDGMENTS

This material is based upon work supported by the U.S. National Science Foundation under Grant No. DMR-92-23546. An acknowledgment is also made to the Donors of the Petroleum Research Fund, administered by the American Chemical Society, and to the U.S. Department of Energy (Division of Materials Sciences, Office of Basic Energy Sciences), under Grant No. DEFG02-91ER45439, for partial equipment and personnel support in connection with the beam line operation. We acknowledge the use of central facilities of the Materials Research Laboratory of the University of Illinois, which is supported by the U.S. Department of Energy (Division of Materials Sciences, Office of Basic Energy Sciences), under Grant No. DEFG02-91ER45439, and the U.S. National Science Foundation under Grant No. DMR-89-20538. The Synchrotron Radiation Center of the University of Wisconsin–Madison is supported by the U.S. National Science Foundation.

*Present address: Applied Materials Inc., Mail Stop 0222, 3050 Bowers Avenue, Santa Clara, CA 95054.

¹See, for example, *Metallic Multilayers and Epitaxy*, edited by M. Hong, D. U. Gubser, and S. A. Wolf (The Metallurgical Society, Warrendale, Pennsylvania, 1988).

²T. Miller, A. Samsavar, G. E. Franklin, and T.-C. Chiang, *Phys. Rev. Lett.* **61**, 1404 (1988).

³M. A. Mueller, T. Miller, and T.-C. Chiang, *Phys. Rev. B* **41**, 5214 (1990).

⁴M. A. Mueller, E. S. Hirschorn, T. Miller, and T.-C. Chiang, *Phys. Rev. B* **43**, 11 825 (1991).

⁵S. Å. Lindgren and L. Walldén, *Phys. Rev. Lett.* **61**, 2894 (1988).

⁶J. E. Ortega, F. J. Himpsel, G. J. Mankey, and R. F. Willis, *Phys. Rev. B* **47**, 1540 (1993).

⁷W. E. McMahon, T. Miller, and T.-C. Chiang, *Phys. Rev. Lett.* **71**, 907 (1993).

⁸S. Å. Lingren and L. Walldén, *J. Phys. Condens. Matter* **1**, 2151 (1989).

⁹T. Miller and T.-C. Chiang, *Phys. Rev. Lett.* **68**, 3339 (1992).

¹⁰M. G. Goldiner, V. B. Sapozhnikov, M. Klaua, and K. Meinel, *J. Phys. Condens. Matter* **3**, 5479 (1991).